

Optimal Reachability with Obstacle Avoidance for Hyper-redundant and Soft Manipulators

Simone Cacace¹, Anna Chiara Lai²  and Paola Loreti²

¹*Dipartimento di Matematica e Fisica, Università degli Studi Roma Tre, Largo S. Murialdo, 1, 00154 Roma, Italy*

²*Dipartimento di Scienze di Base e Applicate per l'Ingegneria, Sapienza Università di Roma, Via A. Scarpa, 16, 00161 Roma, Italy*

Keywords: Soft Manipulators, Hyper-redundant Manipulators, Control Strategies, Reachability, Obstacle Avoidance.

Abstract: We address an optimal reachability problem in constrained environments for hyper-redundant and soft planar manipulators. Both the discrete and continuous devices are inextensible and they are characterized by a bending moment, representing a natural resistance to leave the position at rest, an inequality constraint forcing the bending below a fixed threshold, and a control term prescribing local bending. After introducing the model and characterizing the associated equilibria, we set the problem in the framework of optimal control theory and we present some simulations related to its numerical solution.

1 INTRODUCTION

In this paper, we address an optimal reachability problem in constrained environments for hyper-redundant and soft planar manipulators.

We first consider a planar hyper-redundant manipulator subject to the following constraints and controls on the joint angles: a bending momentum, representing a natural resistance to leave the position at rest, an inequality constraint forcing the joint angles below a fixed threshold, and a control term prescribing each joint angle. Note that the constraints, as well as the controls, are introduced by penalization, i.e., by endowing the Lagrangian of the system with suitable elastic potentials. After an explicit characterization of the equilibria of the system, we state and numerically solve the following stationary optimal control problem: given a target point, find an equilibrium configuration minimizing the tip-target distance and a quadratic cost on the controls, while avoiding a fixed obstacle.

We then address an extension of the model to a continuous setting. The notion of hyper-redundant manipulator is replaced with a soft robot, modelled as an inextensible string subject to a bending moment, a curvature constraint and a pointwise curvature control. Also in this framework, we consider the problem to find an equilibrium configuration whose endpoint

reaches a fixed target in a constrained environment, while minimizing the total curvature. Note that the problem is now stated as a constrained minimization of a cost functional, subject to the ordinary differential equation characterizing the equilibria of the soft manipulator. We also present some numerical simulations exploring this scenario.

The novelty of this paper relies in setting a constrained environment optimal reachability problem in a “soft” fashion, namely by introducing the constraints and controls of the manipulator via angular elastic potentials. The problem was earlier addressed in (Cacace et al., 2020a; Cacace et al., 2019) in an unconstrained framework for both the stationary and the dynamic case. Here, we introduce obstacles in our model, and we discuss the related optimal reachability problems at the equilibrium.

Since their introduction (Chirikjian and Burdick, 1990), hyper-redundant manipulators attracted the interest of researchers due their performances in constrained environments (Michalak et al., 2014). The ability of avoiding obstacles is further enhanced in the framework of soft robotics (Rus and Tolley, 2015; Laschi and Cianchetti, 2014), where the multi-link structure is replaced by a continuous backbone.

We refer to (Chirikjian, 1994) for an early study on the interplay between the continuous and discrete settings. We refer to (Bobrow et al., 1983) for a constrained reachability problem in the framework of optimal control for hyper-redundant manipulators, and

 <https://orcid.org/0000-0003-2096-6753>

to (Wang et al., 2016) for more recent developments. See also the paper (Takács et al., 2015), introducing a control model applied to telesurgical robot systems. Finally we refer to (Thuruthel et al., 2018) for an overview on control of soft manipulators. From the modeling point of view, the present work is mostly inspired by the papers (Jones and Walker, 2006; Laschi et al., 2012; Kang et al., 2011).

The paper is organized as follows. In Section 2, we introduce our model for hyper-redundant manipulators, we study the related equilibria and, in Section 2.2, we address and numerically solve the optimal reachability problem. In Section 3, we extend such approach to a soft manipulator. Finally, in Section 4 we draw our conclusions.

2 HYPER-REDUNDANT MANIPULATORS: MODELING, EQUILIBRIA AND OBSTACLE AVOIDANCE

We consider a control model for a planar, hyper-redundant manipulator whose joints are subject to a bending constraint, a bending moment and a bending control. Such a model was earlier introduced in (Cacace et al., 2020a); here we present its extension to the case of links with non-uniform lengths, we explicitly characterize the related equilibria, and we address an optimal constrained reachability problem in the stationary setting.

2.1 The Control Model and Its Equilibria

We consider a planar manipulator composed by N links and $N + 1$ joints, whose position in the plane is given by the array $q = (q_0, \dots, q_N)$. We assume that $q_0 = (0, 0)$ is an anchor point for the device. We denote by m_k the mass of the k -th joint, for $k = 0, \dots, N$, and we consider negligible the mass of the corresponding links. Moreover, given vectors $v_1, v_2 \in \mathbb{R}^2$, we assume standard notation for the Euclidean norm and the dot product, respectively $|v_1|$ and $v_1 \cdot v_2$, and we define $v_1 \times v_2 := v_1 \cdot v_2^\perp$, where v_2^\perp denotes the clockwise orthogonal vector to v_2 . Finally, the positive part function is denoted by $(\cdot)_+$.

The dynamics of the manipulator is driven by reaction/control forces associated to the following constraints:

1. Inextensibility. The links are rigid and the length

of the k -th link is given by $\ell_k > 0$, namely

$$|q_k - q_{k-1}| = \ell_k \quad k = 1, \dots, N. \quad (1)$$

This constraint is imposed exactly, by introducing for $k = 1, \dots, N$

$$F_k(q, \sigma) := \sigma_k (|q_k - q_{k-1}|^2 - \ell_k^2), \quad (2)$$

where σ_k is a Lagrange multiplier.

2. Angular constraint. We assume that the angle between two consecutive links, say the k -th and the $k + 1$ -th, cannot be greater than a fixed threshold α_k . This can be formalized by the following condition on the joints:

$$(q_{k+1} - q_k) \cdot (q_k - q_{k-1}) \geq \ell_{k+1} \ell_k \cos(\alpha_k).$$

This constraint is imposed via penalization, by introducing, for $k = 1, \dots, N$, the elastic potential

$$G_k(q) := v_k g_k^2(q), \quad (3)$$

where

$$g_k(q) := \left(\cos(\alpha_k) - \frac{1}{\ell_{k+1} \ell_k} (q_{k+1} - q_k) \cdot (q_k - q_{k-1}) \right)_+$$

and $v_k \geq 0$ is a penalty parameter playing the role of an elastic constant.

3. Bending moment. We consider an intrinsic resistance to leave the position at rest (corresponding to null relative angles), introducing the following equality constraint for $k = 1, \dots, N$:

$$b_k(q) := (q_{k+1} - q_k) \times (q_k - q_{k-1}) = 0.$$

The related elastic potential with penalty parameter $\varepsilon_k > 0$ is

$$B_k(q) := \varepsilon_k b_k^2(q). \quad (4)$$

4. Angular control. We prescribe the angle between the joints q_{k-1}, q_k, q_{k+1} for $k = 1, \dots, N$, i.e., the following equality constraint:

$$b_k(q) - \ell_{k+1} \ell_k \sin(\alpha_k u_k) = 0,$$

where $u_k \in [-1, 1]$ is the control term. Note that the control set $[-1, 1]$ is chosen in order to be consistent with the joint angle constraint. Also in this case, we enforce the constraint via penalization, by considering

$$H_k(q, u) := \mu_k (\ell_{k+1} \ell_k \sin(\alpha_k u_k) - b_k(q))^2, \quad (5)$$

where $\mu_k \geq 0$ is a penalty parameter. Note that to set $\mu_k = 0$ corresponds to deactivate the control of the k -th joint and let it evolve according to the remaining constraints only.

The definition of G_k, B_k and H_k in the cases $k = 0$ and $k = N$ is made consistent by considering two ghost joints $q_{-1} := q_0 + (0, \ell_0)$ for some positive ℓ_0 and $q_{N+1} := q_N + (q_N - q_{N-1})$ at the endpoints.

The Lagrangian associated to the hyper-redundant manipulator is then composed by a kinetic energy term and the above discussed elastic potentials:

$$\begin{aligned} \mathcal{L}_N(q, \dot{q}, \sigma, u) := & \sum_{k=0}^N \frac{1}{2} m_k |\dot{q}_k|^2 - F_k(q, \sigma) \\ & - G_k(q) - \frac{1}{2} B_k(q) - \frac{1}{2} H_k(q, u), \end{aligned} \quad (6)$$

where F_k, G_k, B_k and H_k are respectively defined in (2),(3),(4) and (5). Applying the least action principle to the Lagrangian \mathcal{L}_N , one can derive the equations of motion for the manipulator. In particular, equilibria correspond to the solutions of the following stationary system:

$$\begin{cases} \nabla_q \mathcal{L}_N = 0 \\ |q_k - q_{k-1}| = \ell_k & k = 1, \dots, N \\ q_0 = (0, 0) \\ q_{-1} = q_0 + \ell_0(0, 1) \\ q_{N+1} = q_N + (q_N - q_{N-1}) \end{cases} \quad (7)$$

In the next proposition we prove that there exists a unique solution of the above system, characterized by the choice of the control and the model parameters.

Proposition 1. Fix $u \in [-1, 1]^N$, assume $\alpha_k \in [0, \pi/2]$ for $k = 0, \dots, N-1$, define

$$\bar{\alpha}_k := \arcsin \frac{\mu_k}{\varepsilon_k + \mu_k} \sin u_k \alpha_k$$

and, for $k = 1, \dots, N$

$$z_k := -i \sum_{j=1}^k \ell_j e^{i \sum_{h=0}^{j-1} \bar{\alpha}_h}.$$

Then $q = (q_0, q_1, \dots, q_N)$ such that

$$q_k = \begin{cases} (0, 0) & \text{if } k = 0 \\ (\operatorname{Re}(z_k), \operatorname{Im}(z_k)) & \text{if } k = 1, \dots, N \end{cases}$$

is the solution of (7).

Proof. Let q be a solution of (7). Then q satisfies $|q_k - q_{k-1}| = \ell_k$ for $k = 1, \dots, N$, and by construction it is a minimum point for the potential

$$\hat{\mathcal{L}}_N(q) := \sum_{k=0}^N G_k(q) + \frac{1}{2} B_k(q) + \frac{1}{2} H_k(q, u).$$

For $k = 0, \dots, N$, let $\beta_k(q)$ be the angle satisfying

$$\begin{cases} \cos(\beta_k(q)) = (q_{k+1} - q_k) \cdot (q_k - q_{k-1}) / (\ell_k \ell_{k+1}), \\ \sin(\beta_k(q)) = b_k(q) / (\ell_k \ell_{k+1}). \end{cases}$$

Then $\hat{\mathcal{L}}_N$ rewrites

$$\hat{\mathcal{L}}_N(q) = \sum_{k=0}^N \hat{f}_k(\beta_k(q)),$$

where

$$\begin{aligned} \hat{f}_k(\beta) := & \left(\cos(\alpha_k) - \operatorname{sign}(\cos(\beta)) \sqrt{1 - \sin^2(\beta)} \right)^2 \\ & + \frac{\varepsilon_k}{2} \sin^2(\beta) + \frac{\mu_k}{2} \ell_{k+1}^2 \ell_k^2 (\sin(\alpha_k u_k) - \sin(\beta))^2. \end{aligned}$$

Since each term $\hat{f}_k(\beta)$ is positive, then $\beta_k(q)$ minimizes $\hat{f}_k(\beta)$. Clearly, a minimizer $\hat{\beta}$ of $\hat{f}_k(\beta)$ satisfies $\cos(\hat{\beta}) > 0$ and, consequently, $b_k(q)$ is a minimizer of

$$\begin{aligned} f_k(b) := & v_k \left(\cos(\alpha_k) - \sqrt{1 - \frac{1}{(\ell_{k+1} \ell_k)^2} b^2} \right)^2 \\ & + \frac{\varepsilon_k}{2} b^2 + \frac{\mu_k}{2} (\ell_{k+1} \ell_k \sin(\alpha_k u_k) - b)^2. \end{aligned}$$

This implies $f'_k(b_k(q)) = 0$. Also note that, by a direct computation, the minimum is attained in a region where the first additive term of $f_k(b)$ vanishes. We conclude

$$b_k(q) = \ell_{k+1} \ell_k \frac{\mu_k}{\mu_k + \varepsilon_k} \sin \alpha_k u_k = \ell_{k+1} \ell_k \sin \bar{\alpha}_k. \quad (8)$$

Then $\sin(\beta_k(q)) = \sin(\bar{\alpha}_k)$ and this, together with $\cos(\beta_k(q)) \geq 0$, implies

$$(q_{k+1} - q_k) \cdot (q_k - q_{k-1}) = \ell_{k+1} \ell_k \cos \bar{\alpha}_k. \quad (9)$$

Now let q_k^1 and q_k^2 be the components of q_k ; set $z_k := q_k^1 + i q_k^2$ and $v_k := z_k - z_{k-1}$. We then have

$$\begin{aligned} v_{k+1} \bar{v}_k &= (\operatorname{Re}(v_{k+1}), \operatorname{Im}(v_{k+1})) \cdot (\operatorname{Re}(v_k), \operatorname{Im}(v_k)) \\ &+ i (\operatorname{Re}(v_{k+1}), \operatorname{Im}(v_{k+1})) \times (\operatorname{Im}(v_k), \operatorname{Im}(v_k)) \\ &= (q_{k+1} - q_k) \cdot (q_k - q_{k-1}) + i b_k(q) \\ &= \ell_{k+1} \ell_k \cos \bar{\alpha}_k + i \ell_{k+1} \ell_k \sin \bar{\alpha}_k. \end{aligned}$$

Using $\ell_k^2 = \bar{v}_k v_k$ we deduce

$$v_{k+1} = \frac{\ell_{k+1}}{\ell_k} e^{i \bar{\alpha}_k} v_k \quad \forall k = 1, \dots, N$$

and, consequently, also recalling $\ell_0 = 1$,

$$v_k = \ell_k e^{i \sum_{j=0}^{k-1} \bar{\alpha}_j} v_0 \quad \forall k = 1, \dots, N$$

From this (and $v_0 = z_0 - z_{-1} = -i$) we have

$$z_k = z_{k-1} - i \ell_k e^{i \sum_{j=0}^{k-1} \bar{\alpha}_j} \quad \forall k = 1, \dots, N$$

and the thesis follows. \square

By Proposition 1, if $\alpha_k \in [0, \pi/2]$ then the input-to-state map

$$u \mapsto (q_1[u], \dots, q_N[u])$$

associated to (7) reads

$$q_k[u] := \sum_{j=1}^k \ell_j \left(\sin(\theta_j[u]), -\cos(\theta_j[u]) \right) \quad (10)$$

where

$$\theta_j[u] := \sum_{h=0}^{j-1} \bar{\alpha}_h[u]$$

and we recall that

$$\bar{\alpha}_k[u] = \arcsin \frac{\mu_k}{\varepsilon_k + \mu_k} \sin u_k \alpha_k.$$

Remark 1 (On the choice of self-similar ℓ_k). *We remark that, assuming $\sum_{k=0}^{\infty} \ell_k < +\infty$, we can readily extend the above results to the case of an infinite number of joints. For instance, to set $\ell_k = \rho \ell_{k-1}$ for some scaling ratio $\rho \in (0,1)$ models a device with finite total length composed by identical, scaled modules. The kinematic properties of devices characterized by a self-similar structure can be investigated via results in fractal geometry (Lai, 2012), see for instance (Lai et al., 2016) and, for grasping problems, (Lai and Loreti, 2014; Lai and Loreti, 2015).*

2.2 Optimal Reachability with Obstacle Avoidance

Consider the stationary control system (7) and assume for simplicity that the total length of the manipulator is normalized to 1, i.e., $\sum_{k=1}^N \ell_k = 1$. Since the manipulator is composed by a series of rigid, inextensible links, its equilibria configurations can be parametrized by a linear interpolation of its joints coordinates $(q_0[u], \dots, q_N[u])$, denoted by $q(s;u)$, with $s \in [0,1]$.

Here, we address the following optimization problem: to touch a target point in a constrained environment with the end-effector $q(1;u)$, while minimizing a quadratic cost on the controls. More formally, let $q^* \in \mathbb{R}^2$ be a target point, Ω be an open subset of \mathbb{R}^2 representing an obstacle. We consider the following optimization problem:

$$\min J, \quad \text{subject to (7) and to } u \in [-1,1]^N, \quad (11)$$

where

$$J(q,u) := \frac{1}{2} \|u\|_2^2 + \frac{1}{2\delta} |q(1,u) - q^*|^2 + \frac{1}{2\tau} \int_0^1 \text{dist}^2(q(s;u), \Omega^c) ds, \quad (12)$$

δ and τ are positive penalty parameters, and $\|u\|_2$ is the l^2 norm of the control vector u . Note that, due to the particular form of the input-to-state map (10), the function (12) actually depends on u only. In particular, $q(1,u) = q_N[u]$ is the position of the end-effector

Table 1: Global parameter settings for the hyper-redundant manipulator.

Parameter description	Setting
Number of links	$N = 8$
Number of samples	$S = 104$ ($m = 13$)
length of the links	$\ell_k = 1/8$
bending moment	$\varepsilon_k = 10^{-1}(1 - 0.9s_{km})$
curvature control	$\mu_k = 1 - 0.9s_{km}$
penalty	
angle constraint	$\alpha_k = 2\pi(2 + s_{km}^2)$
target point	$q^* = (0.368, -0.085)$
target penalty	$\delta = 10^{-8}$
obstacle penalty	$\tau = 10^{-10}$

of the manipulator, so that the second term in (12) is a penalization of the distance of the tip from the target. On the other hand, the integral term represents the prescription on the whole manipulator (and not only on the joints) of avoiding the obstacle Ω . It is introduced by penalization of the squared distance $\text{dist}^2(\cdot, \Omega^c)$ from the complement of Ω , which is zero if and only if q belongs to the feasible region $\mathbb{R}^2 \setminus \Omega$.

Example 1. *Assume that Ω is the union of M disjoint open balls in \mathbb{R}^2 with centers x_1, \dots, x_M and radii r_1, \dots, r_M . Then*

$$\text{dist}(q, \Omega^c) = \sum_{m=1}^M \max\{0, r_m - |q - x_m|\}.$$

We now numerically solve the optimal control problem (11). To this end, we introduce a discretization on the parametrization interval $[0,1]$ using $S+1$ uniformly distributed samples $s_i = i/S$, for $i = 0, \dots, S$. Here, $S = mN$ is a multiple ($m \gg 1$) of the number of links, so that, for each $k = 0, \dots, N-1$ and $j = 0, \dots, m-1$ we have $q(s_{km+j}; u) = (1 - \lambda_j)q_k[u] + \lambda_j q_{k+1}[u]$, where $\lambda_j = j/m$. Then we approximate the integral term in (12) by a rectangular quadrature rule:

$$\frac{1}{2\tau} \sum_{k=0}^{N-1} \frac{1}{S} \sum_{j=0}^{m-1} \text{dist}^2(q(s_{km+j}; u), \Omega^c).$$

We obtain a fully discrete objective function $J(u)$ with $u \in [-1,1]^N$, and we can solve the problem (11) employing a standard algorithm for finite-dimensional constrained optimization. In our simulations, we use a projected gradient descent method. Moreover, we start with $\tau \gg \delta$ and run the optimization up to convergence, then we slowly decrease τ and repeat the optimization until τ is suitably small. In this way, we first obtain an optimal configuration for the tip-target distance without considering the obstacle. Then, we iterate the procedure, to progressively penalize all the possible interpenetrations with the obstacle. Algorithm 1 summarizes the whole optimization process,

Table 2: Obstacle settings. $B_r(x) \subset \mathbb{R}^2$ denotes the ball of radius r centered in x .

Test	Obstacle
Test 1	$\Omega = \emptyset$
Test 2	$\Omega = B_{0.08}(0.1, -0.35)$
Test 3	$\Omega = B_{0.08}(0.1, -0.35) \cup B_{0.05}(0.3, -0.35)$

where we denote by $\Pi_{[-1,1]^N}(u)$ the projection of u on $[-1, 1]^N$.

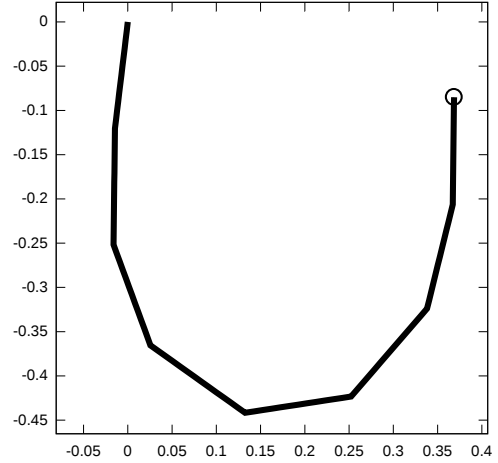
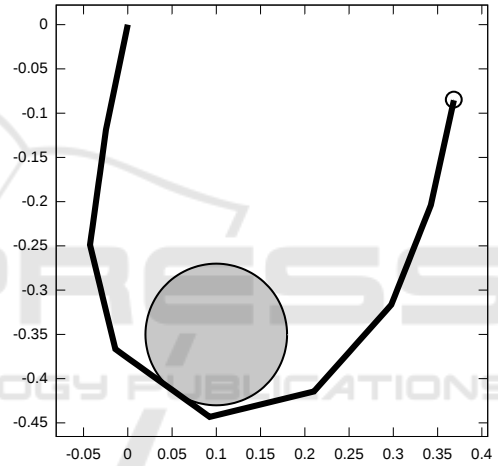
Algorithm 1

- 1: Fix $tol > 0$, $tol_\tau = \tau$, and a step size $0 < \gamma < 1$
 - 2: Assign an initial guess $u^{(0)} \in [-1, 1]^N$
 - 3: Compute $J(u^{(0)})$ and set $J_{imp} = 0$
 - 4: Set $\tau \gg \delta$
 - 5: **repeat**
 - 6: $n \leftarrow 0$, $\tau \leftarrow \tau/2$
 - 7: **repeat**
 - 8: $J_{imp} \leftarrow J(u^{(n)})$
 - 9: Compute $\nabla J(u^{(n)})$
 - 10: $u^{(n)} \leftarrow \Pi_{[-1,1]^N}\{u^{(n)} - \gamma \nabla J(u^{(n)})\}$
 - 11: $n \leftarrow n + 1$
 - 12: Compute $J(u^{(n)})$
 - 13: **until** $|J(u^{(n)}) - J_{imp}| < tol$
 - 14: $u^{(0)} \leftarrow u^{(n)}$
 - 15: **until** $\tau < tol_\tau$
-

The simulation parameters are summarized in Table 1. We compare the cases reported in Table 2, namely the cases in which Ω is the empty set (Test 1), Ω is a ball (Test 2), and Ω is the disjoint union of two balls (Test 3). Note that in Test 1 and Test 2 the target q^* is reached by the end-effector of the manipulator, with clearly different optimal solutions emerging from the differences between the workspaces. On the other hand, in Test 3, we observe that the target is unreachable, since the parameters are set in order to prioritize obstacle avoidance.

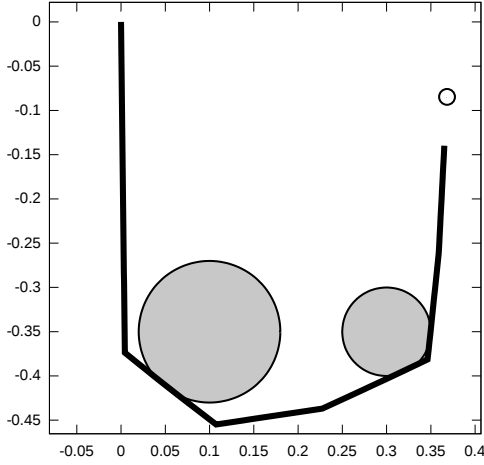
3 AN EXTENSION TO SOFT-MANIPULATORS

In (Cacace et al., 2020a) we introduced a control model for a soft manipulator, obtained as the formal limit (as the number of the joints goes to infinity) of a sequence of the above described hyper-redundant manipulators with fixed unitary length. Roughly speaking, the above introduced angular constraints and controls, prescribing the behaviour of the relative angles of the joints, in the continuum model turn to analogous *curvature* constraints and controls. More precisely, we model the symmetry axis of a planar, inextensible manipulator as an inextensible string with


 Figure 1: The solution q of Test 1.

 Figure 2: The solution q of Test 2.

non-uniform mass distribution. The mass distribution is given by the function $\rho : [0, 1] \rightarrow \mathbb{R}^+$, while the (time-dependent) configuration of the string is given by the function $q : [0, 1] \times [0, +\infty) \rightarrow \mathbb{R}^2$. Then, the evolution of q (and of the corresponding inextensibility multiplier $\sigma : [0, 1] \times [0, +\infty) \rightarrow \mathbb{R}$) is obtained, via the least action principle, by the following continuous counter-part of the Lagrangian introduced in (6):

$$\begin{aligned}
 \mathcal{L}(q, \sigma) := & \int_0^1 \left(\underbrace{\frac{1}{2} \rho |q_t|^2}_{\text{kinetic energy}} - \underbrace{\frac{1}{2} \sigma (|q_s|^2 - 1)}_{\text{inextensibility constr.}} \right. \\
 & - \underbrace{\frac{1}{4} \nu (|q_{ss}|^2 - \omega^2)_+^2}_{\text{curvature constr.}} - \underbrace{\frac{1}{2} \varepsilon |q_{ss}|^2}_{\text{bending moment}} \\
 & \left. - \underbrace{\frac{1}{2} \mu (\omega u - q_s \times q_{ss})^2}_{\text{curvature control}} \right) ds, \quad (13)
 \end{aligned}$$


 Figure 3: The solution q of Test 3.

where q_t, q_s, q_{ss} denote partial derivatives in time and space respectively, $v, \varepsilon, \mu: [0, 1] \rightarrow \mathbb{R}^+$ are the angular elastic constants associated, respectively, to the curvature constraint, the bending moment and the curvature control, and $u: [0, 1] \times [0, +\infty) \rightarrow [-1, 1]$ is the curvature control. For a comparison between the discrete and continuous model we refer to (Cacace et al., 2020b), while for a description and some parameter tuning of the projection of the three dimensional model to its symmetry axis we refer to (Cacace et al., 2019).

The equilibria of the system associated with the Lagrangian (13) were explicitly characterized in (Cacace et al., 2020a). In particular, assuming the technical condition $\mu(1) = \mu_s(1) = 0$, the shape of the manipulator at the equilibrium is the solution q of the following second order controlled ODE:

$$\begin{cases} q_{ss} = \bar{\omega} u q_s^\perp & \text{in } (0, 1) \\ |q_s|^2 = 1 & \text{in } (0, 1) \\ q(0) = (0, 0) \\ q_s(0) = (0, -1). \end{cases} \quad (14)$$

where $\bar{\omega} := \mu\omega/(\mu + \varepsilon)$.

Remark 2 (On the equilibria in discrete and continuous settings). *We recall that, since q is parametrized in arc-length coordinates, the quantity $\kappa := q_{ss} \times q_s$ is the signed curvature of q . Now, by dot-multiplying q_s^\perp in both sides of the first equation of (14) we obtain the condition $q_{ss} \times q_s = \bar{\omega}u$: we point out the symmetry with the condition (8) on the angle between consecutive joints of the manipulator at the equilibrium.*

Also note that, for a fixed $u \in C^2([0, 1])$, (14) admits a unique classical solution, given explicitly by

$$q(s) = \int_0^s \left(\sin(\theta(\xi)), -\cos(\theta(\xi)) \right) d\xi \quad (15)$$

where

$$\theta(\xi) := \int_0^\xi \bar{\omega}(z)u(z) dz \quad \text{and} \quad \bar{\omega}(s) := \frac{\mu(s)\omega(s)}{\mu(s) + \varepsilon(s)}.$$

We remark the analogy with the discrete input-to-state map (10).

3.1 Optimal Reachability with Obstacle Avoidance in the Continuous Setting

In this section we address the static optimal reachability problem, discussed in Section 2.2, in the framework of soft robotics. More precisely, given an obstacle $\Omega \subset \mathbb{R}^2$ and a target point $q^* \in \mathbb{R}^2 \setminus \Omega$, we consider the optimal control problem:

$$\min \mathcal{J}, \quad \text{subject to (14) and to } |u| \leq 1, \quad (16)$$

where

$$\begin{aligned} \mathcal{J}(q, u) := & \frac{1}{2} \int_0^1 u^2(s) ds + \frac{1}{2\delta} |q(1) - q^*|^2 \\ & + \frac{1}{2\tau} \int_0^1 \text{dist}^2(q(s), \Omega^c) ds, \end{aligned} \quad (17)$$

with $\delta, \tau > 0$. As in (12), the cost functional has three components: a quadratic cost on the controls, a tip-target distance and an integral term, vanishing if and only if there is no interpenetration with the obstacle Ω . Similarly to the discrete case, this term encompasses the obstacle avoidance task as $\tau \rightarrow 0$. Moreover, the input-to-state map (15) allows to reduce \mathcal{J} to a functional depending on the control u only.

Discretization and optimization are performed as in the case of hyper-redundant manipulators, using quadrature rules to approximate the integrals appearing in the input-to-state map (15) and in the functional (17).

For the sake of comparison, we adopt the same obstacle settings of the discrete case, reported in Table 2. The other global parameter settings are in Table 3. We note that in Test 1 and Test 2 the target is reached and the optimal controlled curvature κ is far below the fixed threshold $\bar{\omega}$ – see Figure 4 and Figure 5. Adding a further obstacle (Test 3) shows more clearly the impact of curvature and obstacle avoidance constraints on the optimization process: the optimal configuration fails in reaching the target – see Figure 6.

4 CONCLUSIONS

In this paper we investigated optimal reachability problems in constrained environments for hyper-redundant and soft manipulators. From a modeling

Table 3: Global parameter settings for the soft manipulator.

Parameter description	Setting
Quadrature nodes	$N = 100$
Discretization step	$\Delta_s = 1/N = 0.01$
bending moment	$\varepsilon(s) = 10^{-1}(1 - 0.9s)$
curvature control	$\mu(s) = 1 - 0.9s$
penalty	
curvature constraint	$\omega(s) = 2\pi(2 + s^2)$
target point	$q^* = (0.368, -0.085)$
target penalty	$\delta = 10^{-8}$
obstacle penalty	$\tau = 10^{-10}$

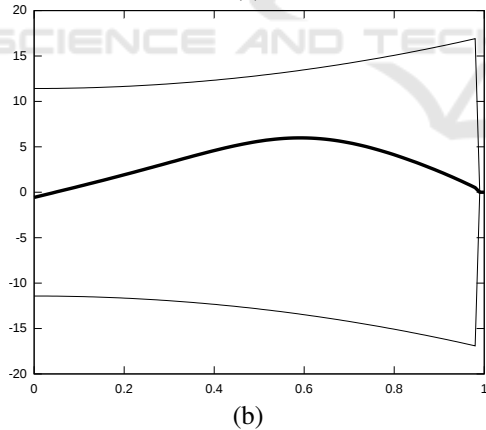
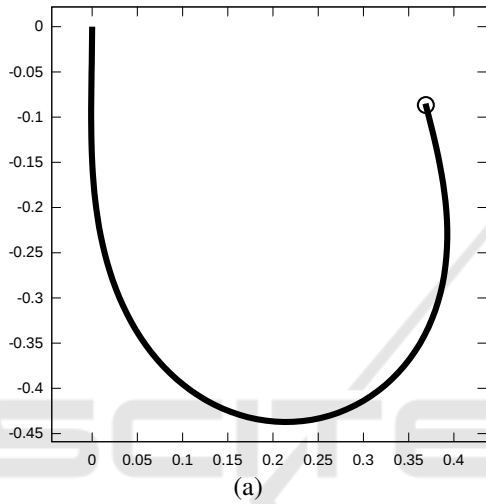


Figure 4: In (a) the solution q of Test 1, in (b) the related signed curvature $\kappa(s)$ (bold line) and curvature constraints $\pm\bar{\omega}$ (thin lines).

point of view, the discrete and continuous settings share inextensibility, an intrinsic resistance to bending, the prohibition to bend over a fixed threshold, and the control on the relative angles/curvature of the device. The inextensibility constraint is introduced exactly, while the bending constraints are modelled as internal reaction forces, thus introduced via penaliza-

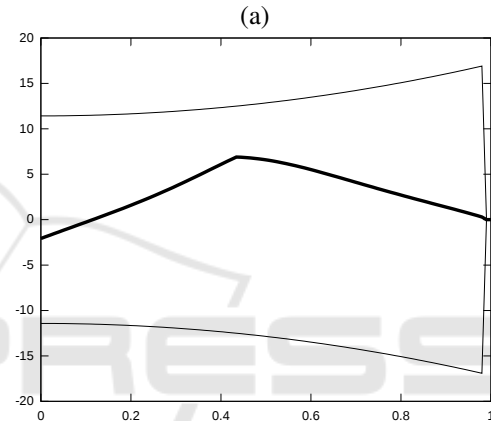
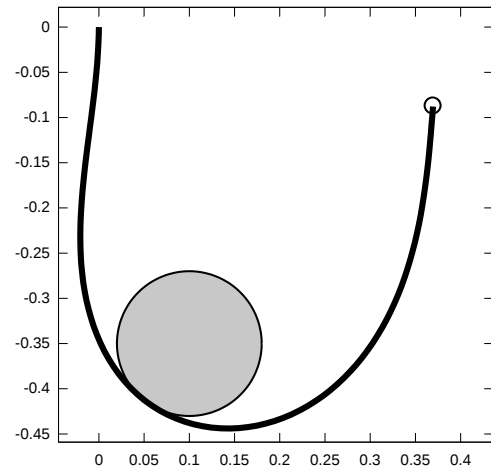


Figure 5: In (a) the solution q of Test 2, in (b) the related signed curvature $\kappa(s)$ (bold line) and curvature constraints $\pm\bar{\omega}$ (thin lines).

tion. After characterizing the equilibria of the corresponding systems, we addressed a stationary optimal control problem. It consists in reaching a fixed target while avoiding an obstacle, and minimizing a quadratic cost on the controls. The paper is completed with numerical simulations showing some optimal solutions in both discrete and continuous cases.

The main contribution consists in the investigation of obstacle avoidance for a recent model (introduced by the authors in (Cacace et al., 2020a)) in the framework of optimal control theory.

We plan to extend the present approach to the investigation of dynamic optimal controls in the context of grasping and obstacle avoidance. We aim to synthesize dynamic controls for both optimal power grasping and fine manipulation.

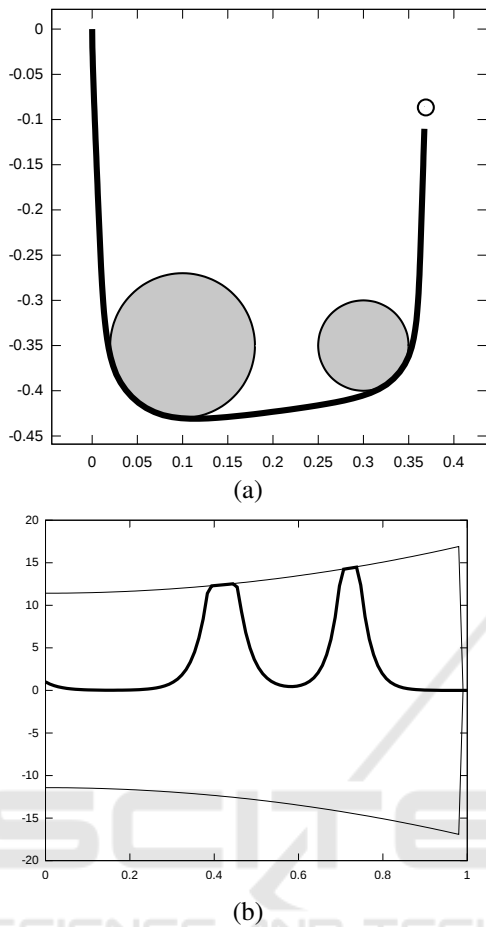


Figure 6: In (a) the solution q of Test 3, in (b) the related signed curvature $\kappa(s)$ (bold line) and curvature constraints $\pm\bar{\omega}$ (thin lines).

REFERENCES

- Bobrow, J. E., Dubowsky, S., and Gibson, J. (1983). On the optimal control of robotic manipulators with actuator constraints. In *1983 American Control Conference*, pages 782–787. IEEE.
- Cacace, S., Lai, A. C., and Loreti, P. (2019). Control strategies for an octopus-like soft manipulator. In *2019 - Proceedings of the 16th International Conference on Informatics in Control, Automation and Robotics (ICINCO)*, volume 1, pages 82–90. IEEE.
- Cacace, S., Lai, A. C., and Loreti, P. (2020a). Modeling and optimal control of an octopus tentacle. *SIAM Journal on Control and Optimization*, 58(1):59–84.
- Cacace, S., Lai, A. C., and Loreti, P. (2020b). Optimal reachability and grasping for a soft manipulator. *preprint, arXiv 2002.05476*.
- Chirikjian, G. S. (1994). Hyper-redundant manipulator dynamics: A continuum approximation. *Advanced Robotics*, 9(3):217–243.
- Chirikjian, G. S. and Burdick, J. W. (1990). An obstacle avoidance algorithm for hyper-redundant manipulators. In *Proceedings., IEEE International Conference on Robotics and Automation*, pages 625–631. IEEE.
- Jones, B. A. and Walker, I. D. (2006). Kinematics for multisection continuum robots. *IEEE Transactions on Robotics*, 22(1):43–55.
- Kang, R., Kazakidi, A., Guglielmino, E., Branson, D. T., Tsakiris, D. P., Ekaterinaris, J. A., and Caldwell, D. G. (2011). Dynamic model of a hyper-redundant, octopus-like manipulator for underwater applications. In *Intelligent Robots and Systems (IROS), 2011 IEEE/RSJ International Conference on*, pages 4054–4059. IEEE.
- Lai, A. C. (2012). Geometrical aspects of expansions in complex bases. *Acta Mathematica Hungarica*, 136(4):275–300.
- Lai, A. C. and Loreti, P. (2014). Robot’s hand and expansions in non-integer bases. *Discrete Mathematics & Theoretical Computer Science*, 16(1).
- Lai, A. C. and Loreti, P. (2015). Self-similar control systems and applications to zygodactyl bird’s foot. *Netw. Heterog. Media*, 10(2):401–419.
- Lai, A. C., Loreti, P., and Vellucci, P. (2016). A Fibonacci control system with application to hyper-redundant manipulators. *Mathematics of Control, Signals, and Systems*, 28(2):15.
- Laschi, C. and Cianchetti, M. (2014). Soft robotics: new perspectives for robot bodyware and control. *Frontiers in Bioengineering and Biotechnology*, 2:3.
- Laschi, C., Cianchetti, M., Mazzolai, B., Margheri, L., Follador, M., and Dario, P. (2012). Soft robot arm inspired by the octopus. *Advanced Robotics*, 26(7):709–727.
- Michalak, K., Filipiak, P., and Lipinski, P. (2014). Multi-objective dynamic constrained evolutionary algorithm for control of a multi-segment articulated manipulator. In *International Conference on Intelligent Data Engineering and Automated Learning*, pages 199–206. Springer.
- Rus, D. and Tolley, M. T. (2015). Design, fabrication and control of soft robots. *Nature*, 521(7553):467–475.
- Takács, Á., Kovács, L., Rudas, I., Precup, R.-E., and Haidegger, T. (2015). Models for force control in telesurgical robot systems. *Acta Polytechnica Hungarica*, 12(8):95–114.
- Thuruthel, G. T., Ansari, Y., Falotico, E., and Laschi, C. (2018). Control strategies for soft robotic manipulators: A survey. *Soft robotics*, 5(2):149–163.
- Wang, B., Wang, J., Zhang, L., Zhang, B., and Li, X. (2016). Cooperative control of heterogeneous uncertain dynamical networks: An adaptive explicit synchronization framework. *IEEE transactions on cybernetics*, 47(6):1484–1495.